Vol. 29 (1998) *ACTA PHYSICA POLONICA B* No 7

BOSE–EINSTEIN CORRELATIONS IN THE LUND MODEL* , **

Bo Andersson

Department of Theoretical Physics, Lund University
Sölvegatan 14A, S-223 62 Lund, Sweden
e-mail: bo@thep.lu.se

(Received February 16, 1998)

I will present the Lund Model fragmentation in a somewhat different way than what is usually done. It is true that the formulas are derived from (semi-)classical probability arguments, but they can be motivated in a quantum mechanical setting and it is in particular possible to derive a transition matrix element. I will present two scenarios, one based upon Schwinger tunneling and one upon Wilson loop operators. The results will coincide and throw some light upon the sizes of the three main phenomenological parameters which occur in the Lund Model. After that I will show that in this way it is possible to obtain a model for the celebrated Bose–Einstein correlations between two bosons with small relative momenta. This model will exhibit non-trivial two- and three-particle BE correlations, influence the observed ρ-spectrum and finally be different for charged and neutral pion correlations.

PACS numbers: 13.87. Fh

1. Introduction

We have after many years of hard work learned that the results from the experimental analysis of multiparticle production can be well described in terms of a coherent partonic cascade, [1,2], followed by a hadronization process. This is particularly so for the e^+e^--annihilation processes, which I will use as example in this talk. There is further a very similar picture emerging in the deep inelastic scattering experiments from HERA (and maybe also from the purely hadronic hard scattering events seen in FERMILAB).

* Presented at the XXXVII Cracow School of Theoretical Physics, Zakopane, Poland, May 30–June 10, 1997.
** Report on Work done together with M. Ringnér

The treatment of the partonic cascades requires the use of some quantum mechanics, at least for the interference patterns between different gluon radiation patterns. As I will show in my second lecture, these processes have nevertheless a great similarity to the results in classical hydrodynamical flow situations. The hadronization parts are on the other hand usually treated in terms of semi-classically motivated stochastic processes. In this lecture I will show that at least in the Lund Model, [3], it is possible to consider the results inside a quantum mechanically motivated framework. Viewed in that way most of the results of the Lund Model can be understood in "the ordinary language" and thus be related to the classical results obtained in earlier models.

One basic motivation for a quantum mechanical treatment is the observation of the Hanbury-Brown–Twiss effect, [4], (which I will, as is usually done, term "Bose–Einstein Correlations", (BEC)) in bosonic distributions. The ideas of BEC originated in astronomy where one uses the interference pattern of the photons to learn about the size of the photon emission region, *i.e.* the size of the particular star, which is emitting the light. The effect can be described as an enhancement of the two-particle correlation function that occur when the two particles are identical bosons and have very similar energy-momenta. To obtain such a result it is in general necessary to invoke the wave-patterns of the quanta, [6].

There are, however, at least one possibility to obtain the (two-particle) BEC in terms of a classically motivated process. Sjöstrand has introduced a clever device as a subroutine to JETSET, in which the HBT effect is simulated as a mean field potential attraction between identical bosons [5]. Thus, given a set of energy-momentum vectors of identical bosons, $p_1, \ldots, p_n$, generated without any BEC effect, it is possible to reshuffle the set into another set where each pair on the average has been moved relatively closer to show a (chosen) BEC distribution, while still keeping to energy-momentum conservation for the whole event.

A well-known formula [6] to relate the two-particle correlation function (in four-momenta $p_j, j = 1, 2$ with $q = p_1 - p_2$) to the space-time density distribution, ρ, of (chaotic) emission sources is,

$$\frac{\sigma d^2\sigma_{12}}{d\sigma_1 d\sigma_2} = 1 + |\mathcal{R}(q)|^2\,, \tag{1}$$

where $\mathcal{R}$ is the normalized Fourier transform of the source density

$$\mathcal{R}(q) = \frac{\int \rho(x)dx \exp(iqx)}{\int \rho(x)dx}\,. \tag{2}$$

This quantity is often, without very convincing reasons, parametrized in terms of a "source radius" R and a "chaoticity parameter" λ,

$$|\mathcal{R}(q)|^2 = \lambda \exp(-R^2 Q^2) \tag{3}$$

with $Q^2 = -q^2$. The source radii obtained by this parametrization tend to be similar in all hadronic interactions (we exclude heavy ion interactions where the extensions of nuclear targets and probes will influence the result), with $R \sim 0.5 - 1$ fm, but the chaoticity varies rather much depending upon the particular data sample and the method of the fit. At present the knowledge of higher-order correlations is still limited in the experimental data, although, as I will stress, there should be such correlations and the observation of them is not only a definite prediction but also a decisive test for the model I am going to present.

The first attempt to provide the Lund Model with a quantum mechanical framework is a method devised in [7]. In particular there is instead of a probability distribution for the hadrons a production matrix element with well-defined phases. This was then be used to make a model of the HBT effect. Although this model stems from different considerations it will nevertheless contain predictions which are similar to those in the ordinary approach giving Eq. (1). The correlations are implemented as weights assigned to events generated by JETSET. One motivation for this new effort, performed together with my student Markus Ringnér, was to extend the model to the general situation when there are several kinds of bosons as well as many particles of each kind. Another was to obtain a more precise understanding of the (at that time) somewhat cavalier assumptions behind the ideas in [7]. (Or as one of my friends told me: "You are allowed to play around for most parts of your life but at least at some time you ought to behave in a serious way". I do not feel serious yet but I am nevertheless curious).

In the next section I will survey those features of the Lund model, that are necessary for the following and also make a connection to Feynman graphs for multiparticle production as well as the results of Regge theory. After that I will present the BEC model and apply it to situations where there are many (n) identical bosons. The resulting expressions contain a sum of in general $n!$ terms, *i.e.* it is of exponential type from a computational point of view. It is possible to subdivide the expressions in accordance with the group structure of the permutation group. Although the higher order terms provide small contributions in general the computing times are still forbidding. In order to speed up the calculations we have instead introduced the notion of *links* between the particles. In this way it is possible to obtain expressions of a power type from a calculational point of view, which are perfectly tractable in a computer.

I will end with a set of results and predictions from the model but the main reason for this talk is to present the basic ideas. For those who are interested in the details of "how it works" there is a Monte Carlo simulation program available from Markus (markus@thep.lu.se).

2. Some features of the Lund hadronization model

In the Lund string model the basic quantity is the confining color field which is spanned between the (original) $q\bar{q}$-pair via the color-connected gluons. It is approximated by some particular modes of the massless relativistic string where the endpoints of the string are identified with the q and $\bar{q}$ and where the gluons are assumed to behave as internal excitations on the string. The string can break up into smaller pieces by the production of $q\bar{q}$-pairs (*i.e.* new endpoints). Such a pair will immediately start to separate because of the string tension, which in the rest frame of a string segment corresponds to a constant force κ; phenomenologically $\kappa \simeq 1$ GeV/fm. Final state mesons are formed from a q and a $\bar{q}$ from adjacent vertices, as shown in Fig. 1.

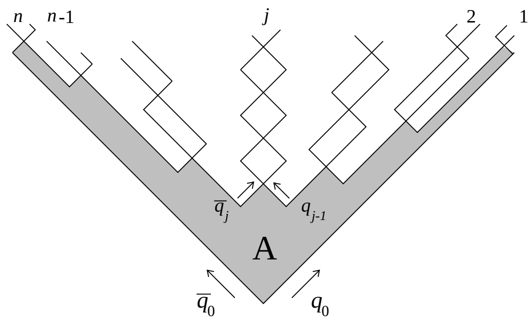

Fig. 1. The decay of a Lund Model string

Each breakup vertex will separate the string into two causally disconnected parts. From the causality, together with Lorentz covariance and straightforward kinematics, it is possible to derive a unique breakup rule for the string by means of (semi-)classical arguments [8].

The unique breakup rule results in the following (non-normalized) probability for a string to decay into the hadrons $(p_1, \ldots, p_n)$.

$$dP(p_1, \ldots, p_n) = \left[\prod_i (N dp_i \delta(p_i^2 - m_i^2))\right] \delta\left(\sum_j p_j - P_{\text{tot}}\right) \exp(-bA)\,, \quad (4)$$

where A is the area of the breakup region as indicated in Fig. 1 and N and b are two parameters. Actually as we will find below the parameter b can be given a fundamental color dynamical interpretation, while N plays the role of a "density" for the hadronic states (and it will in particular contain also the transverse momentum fluctuations "out of the string plane" if dp_i is a four-dimensional energy-momentum space region).

Before I continue I would like to remark that this picture may seem very different from the ordinary Feynman diagramatics language in multiparticle production. Nevertheless in reality it is conceptually very similar. To see that consider anyone of the vertices, *e.g.* the one from which the $\bar{q}_j$ is stemming in Fig. 1. We assume that it has lightcone coordinates (x_{+j}, x_{-j}) in a frame where the origin is $(0, 0)$ and the original q_0 and $\bar{q}_0$ have (lightcone) energy momenta $(P_+, 0)$ and $(0, P_-)$ (with $P_+P_- = s$, the cms energy squared).

Then the above-mentioned partitioning at the vertex j corresponds to a separation of the whole event into two groups of particles, denoted $(1, \ldots, j)$ and $(j + 1, \ldots, n)$ in Fig. 1, with energy-momenta $(P_+ - \kappa x_{+j}, \kappa x_{-j})$ and $(\kappa x_{+j}, P_- - \kappa x_{-j})$. These two particle jets move roughly along the q_0 and $\bar{q}_0$ directions, respectively. Pictorially this can be described as in Fig. 2, *i.e.* the $(q_0, \bar{q}_0)$ are transferred to the two final state groups with a momentum transfer between them of the size $q = (\kappa x_{+j}, -\kappa x_{-j})$ (the sign determined by the way we have drawn its direction; it must as all momentum transfers be a space-like vector).

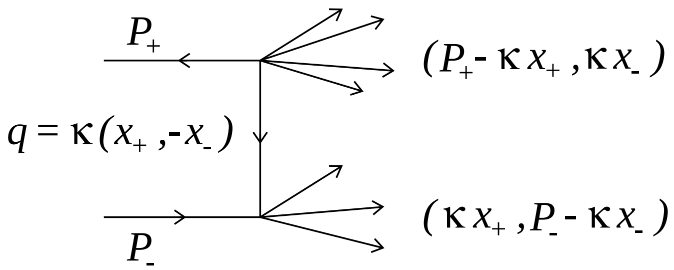

Fig. 2. The space-time picture with a production vertex at (x_+, x_-) is dual to a momentum space picture similar to a Feynman graph with a momentum transfer $q = (\kappa x_+, -\kappa x_-)$ between the particles produced "to the left" and "to the right" of the space-time vertex.

It does not take much thought to understand that the same construction can be made at any vertex and that *the vertex positions in space-time in this way corresponds to the momentum transfers in energy-momentum space between the final state particles.* Therefore the area fragmentation law can be related in a unique way to a description in terms of a multiperipheral ladder graph with production vertices for the on-shell particles, $\{p\}_j$, and with propagators, $\{q\}_j$, between these vertices. The whole situation in the ladder graph is in a precise way dual to the space-time description in Eq. (4) and Fig. 1.

I will not write out the corresponding "local" formulas but we may deduce the general properties directly from the "global" Eq. (4). We firstly note that it contains a phase space factor, which in order to give large contributions will require many particles. On the other hand the negative area exponential will similarly tend to suppress large production regions. There is an evident compromise in terms of the area below a "typical" hyperbola. The area would then be $|Q^2|\Delta y$ with $|Q^2| \simeq 1/b$ ($\simeq 1.5$ GeV^2 phenomenologically) and with $\Delta y = \log(s/s_0)$, where s_0 is a scale of the order of a typical hadronic mass squared. We can go further and show that in this typical hyperbola decay we obtain $\langle n \rangle \simeq \Delta y/\rho$ particles with a a rapidity density $\rho \simeq |Q^2|/s_0$. There will not be any large subenergies $(p_j + p_{j+1})^2$ (large rapidity gaps means "loss of entropy" from the phase space factor) and the momentum transfers are evidently limited (inclusively the distribution in proper time τ, which is related to the momentum transfer as $\tau = |Q|/\kappa$ of the vertices $\tau^2 = x_{+j}x_{-j} \equiv |Q_j^2|/\kappa^2$ is a gamma-distribution governed by the b-parameter).

For such a model all the arguments from the old multiperipheral models (and also those of Gribov to obtain Regge behaviour from unitarity) works. We obtain easily that the total probability for any multiparticle state in the Lund Model is a power in the cms energy $\sum_n \int dP(p_1, \ldots, p_n) \simeq s^a$. The parameter a is determined from a ("local", *i.e.* involving a single vertex) integral equation (once again as in the unitarity equations, *etc*). It should come as no surprise that the parameter values we obtain for $a \simeq 0.5$ and for b correspond to the ρ trajectory intercept and slope, respectively. After all it is the light u and d flavors which are overwhelmingly produced in the Lund Model!

All of these considerations might, of course, motivate an interpretation of the Lund Model results in terms of "ordinary" quantum mechanical production formulas. The key is to reconsider the result in Eq. (4), which was derived from (semi-)classical probability concepts in [8], in terms of Fermi's golden rule, *i.e.* that the transition probability is the final state phase space multiplied by the square of a transition amplitude $|\mathcal{M}|^2$. In the next section I will provide such motivations for interpreting the negative area exponential as the square of a matrix element. There are at least two possible mechanisms, *viz.* a quantum mechanical tunneling process a la Schwinger and/or the possible relationship to the Wilson loop operators in a gauge field theory. We will find that they provide very similar answers to the problem.

3. Schwinger tunneling and Wilson loop operators

We note that while a massless $q\bar{q}$-pair without transverse momentum can be produced in a point-like way anywhere along the string, a massive pair or a pair with transverse momentum must classically be produced at a distance so that the string energy between them can be used to fulfil energy-momentum conservation. If the transverse momentum is conserved in the production process, *i.e.* the $q\bar{q}$ with masses μ obtain $\pm\vec{k}_\perp$, respectively, then the pair may classically be realized at a distance $\delta x = 2\mu_\perp/\kappa$, where $\mu_\perp$ is the transverse mass $\sqrt{\mu^2 + \vec{k}_\perp^2}$.

The probability for a quantum mechanical fluctuation of a pair, occurring with $\mu_\perp$ at the (space-like) distance δx, is in a force-free region given by the free Feynman propagator squared:

$$|\Delta_{\mathrm{F}}(\delta x, \mu_\perp)|^2 \sim \exp(-2\mu_\perp \delta x) = \exp\left(-\frac{4\mu_\perp^2}{\kappa}\right) . \tag{5}$$

A corresponding quantum mechanical tunneling process in a constant force field will according to WKB methods give

$$\left|\exp\left(-\int_0^{\delta x} \sqrt{\mu_\perp^2 - (\kappa x)^2 dx}\right)\right|^2 = \exp\left(-\frac{\pi\mu_\perp^2}{\kappa}\right) \equiv P(\mu_\perp) . \tag{6}$$

The difference is that in the force-free case we obtain an exponential suppression $4\mu_\perp^2/\kappa$ but when the constant force pulls the pair apart we obtain the somewhat smaller suppression $\pi\mu_\perp^2/\kappa$. Besides the mass suppression (which phenomenologically will suppress strange quark-pairs with a factor of ~ 0.3 compared to "massless" up and down flavored pairs) we obtain the transverse momentum Gaussian suppression

$$\exp\left(-\frac{1}{2\sigma^2} k_\perp^2\right) \quad \text{with} \quad 2\sigma^2 = \frac{\kappa}{\pi} . \tag{7}$$

The value of σ as used in JETSET is a bit larger than the result in Eq. (7) but this can be understood as an effect of soft gluon generation along the string. The transverse momentum of a hadron produced in the Lund Model is then the sum of the transverse momenta of its constituents.

We may use the elementary result in Eq. (6) to calculate the persistence probability of the vacuum, $\mathcal{P}$, as it is defined in [9]. It is the probability that the no-particle vacuum will not break up, owing to pair-production, during the time T over a transverse region $A_\perp$, when a constant force κ is applied along the longitudinal x-direction over a region L:

$$\mathcal{P} = \prod_{t\in(0,T),x\in(0,L),\vec{k}_\perp,s,f} (1 - P(\mu_\perp)) = \exp\left(\sum_{t,x,\vec{k}_\perp,s,f} \log(1-P)\right). \qquad (8)$$

We have then assumed that the field couples to (fermion) pairs with spin s and flavors f and we sum over all possibilities for the production. As each pair needs a longitudinal size $\delta x = 2\mu_\perp/\kappa$ and, according to Heisenberg's indeterminacy relation, will live during a time-span $2\pi/2\mu_\perp$ there is at most $\kappa LT/2\pi$ pairs possible over the space-time region LT. The transverse momentum summation can be done by Gaussian integrals from an expansion of $\log(1-P)$ and the introduction of the well-known number of waves available in a transverse region $A_\perp$: $(A_\perp/(2\pi)^2)d^2k_\perp$. In this way we obtain for the persistence probability

$$\mathcal{P} = \exp(-\kappa^2 LTA_\perp \Pi) \quad \text{with} \quad \Pi = \frac{n_f n_s}{4\pi^3}\sum_{n=1}^{\infty}\frac{1}{n^2}\exp\left(-\frac{n\pi\mu^2}{\kappa}\right), \qquad (9)$$

where n_f, n_s is the number of flavor and spin states.

There are two remarks to this result. Firstly, although the method to treat the integration over time and longitudinal space, by close-packing reasonably sized boxes, may not seem convincing the final formula in Eq. (9) coincides with the one obtained by Schwinger [10], for the case of a constant electric field $\mathcal{E}$. Then κ is identified with the force of the charges in the external field, *i.e.* $\kappa \to e\mathcal{E}$.

Secondly, the result is in evident agreement with the formula for the decay of the Lund string in Eq. (4) if we identify LT with the (coordinate space) area size A. In this way we also obtain the result that the parameter b is

$$b = \kappa^2 A_\perp \Pi\,, \qquad (10)$$

i.e. it corresponds to the transverse size of the (constant) force field, which we have modeled by the string. The quantity Π is $1/(12\pi)$ for two massless spin 1/2-flavors.

The second quantum mechanical approach is to note that a final state hadron stems from a q from one vertex j and a $\bar{q}$ from the adjoining vertex $j+1$. In order to keep to gauge invariance it is then necessary that the production matrix element contains at least a gauge connector between the vertices: $\exp(i\int_j^{j+1} g\mathcal{A}^\mu dx_\mu)$, where g is the charge and $\mathcal{A}^\mu$ the gauge field. Consequently the total production matrix element must contain (at least) a

Wilson loop operator:

$$\mathcal{M} = \exp(i \oint g\mathcal{A}^{\mu} dx_{\mu}) \tag{11}$$

with the integration around the region A (note that the field is singular along the border line and we are therefore not allowed to distort the integration contour inwards). The operator in Eq. (11) was predicted (and inside lattice gauge calculations also found) to behave as

$$\mathcal{M} = \exp(i\xi A) \tag{12}$$

with the real part of ξ, $\mathrm{Re}(\xi) = \kappa$. In the present situation where the force field region decays we expect an imaginary part, corresponding to the pair production rate according to the well-known Kramers–Kronig [11] relationship for the dielectricity in matter, in this case the QCD vacuum.

Before I continue let me make a few remarks on the notion of "gauge-connector". It is well-known that (local) gauge transformations (with the gauge function $\Lambda(x)$) are implemented in such a way that while the vector potential field $\mathcal{A}^{\mu} \to \mathcal{A}^{\mu} + \partial\Lambda/\partial x_{\mu}$ the corresponding fermion fields obtain a phase change $\psi \to \psi \exp(ig\Lambda)$. This means that a theory where $\mathcal{A}^{\mu}$ is coupled to a conserved current is gauge invariant (for a non-abelian theory like QCD some care must be exercised; the "conservation of the current", just as *e.g.* "unitarity" is in Feynman language taken care of by the introduction of formal "ghost" field compensations).

Further, fermion quantities like $\bar{\psi}O\psi$ (with O a Dirac matrix) evaluated in the same point are then obviously gauge invariant. But *this does not apply to situations when the fermion–antifermio pair stem from different production points.* Then the gauge connector, which was introduced by Schwinger, is a necessity. A use of Stoke's theorem tells us that the quantity ξ in Eq. (12) is for a loop with a space-like (time-like) normal the magnetic (electric) field flux through the loop. It is multiplied by the effective charge and consequently it will therefore be influenced by the dielectricity of the vacuum which is governed by the pair production rate (for the non-abelian QCD this means a "running" as we will soon find).

The two interpretations of the area law, *i.e.* the Schwinger tunneling in Eq. (9) and the Wilson loop operator result in Eq. (12) can be related if we note that according to Gauss' Law the integral over the extension of the force field should correspond to the charge. For a thin string we should then obtain for the area falloff rate $b \propto \kappa^2 A_{\perp} \propto \kappa\alpha$. Although Gauss' law is more complicated for a non-abelian field with triplet and octet color-charges and similarly octet fields it is possible to make a case for an identification of the parameter b (expressed in energy-momentum space units) as

$$b = \frac{n_f \bar{\alpha}}{12\kappa} \tag{13}$$

which is what we should expect from the expected imaginary part of the dielectricity in Eq. (12) ($\bar{\alpha} = 3g^2/(4\pi)$ is then the effective QCD coupling, including the color factors). The result is also phenomenologically supported if we consider a partonic cascade down to a certain transverse momentum cutoff $k_{\perp c}$ and then use the Lund Model hadronization formulas to obtain the observed properties of the final state. In that way we may determine the parameters in the model as functions of the partonic cascade cutoff. A remarkably good fit to the b-parameter is given by $C/\log(k_{\perp c}^2/\Lambda^2)$ with C according to Eq. (13) (thereby including the QCD running coupling) and $\Lambda \simeq .5$ GeV [12].

Independently of the precise identification of b, we obtain a possible matrix element from Eq. (12), again with A expressed in space-time units

$$\mathcal{M} = \exp(i\kappa - b\kappa^2/2)A \tag{14}$$

which not only will provide us with the Lund decay probability in Eq. (4), but also can be used in accordance with [7] to provide a model for the BEC effect for the correlations among identical bosons.

4. The Bose Einstein Correlation Model

We now consider a final state containing (among possibly a lot of other stuff) n identical bosons. There are $n!$ ways to produce such a state, each corresponding to a different permutation of the particles. According to quantum mechanics the transition matrix element is to be symmetrized with respect to exchange of identical bosons. This leads to the following general expression for the production amplitude

$$\mathcal{M} = \sum_{\mathcal{P}} \mathcal{M}_{\mathcal{P}}\,, \tag{15}$$

where the sum goes over all possible permutations $\mathcal{P}$ of the identical bosons. The cross section will then contain the square of the symmetrized amplitude $\mathcal{M}$

$$|\mathcal{M}|^2 = \sum_{\mathcal{P}} \left(|\mathcal{M}_{\mathcal{P}}|^2 \left(1 + \sum_{\mathcal{P}' \neq \mathcal{P}} \frac{2\mathrm{Re}(\mathcal{M}_{\mathcal{P}}\mathcal{M}^*_{\mathcal{P}'})}{|\mathcal{M}_{\mathcal{P}}|^2 + |\mathcal{M}_{\mathcal{P}'}|^2} \right) \right). \tag{16}$$

In the JETSET scheme the probability to obtain the final state configuration would be given by

$$|\mathcal{M}|^2 = \sum_{\mathcal{P}} |\mathcal{M}_{\mathcal{P}}|^2 \tag{17}$$

instead of the probability in Eq. (16). Comparing Eq. (16) and Eq. (17) we find that the quantum mechanical symmetrization can be introduced by weighting the produced event with

$$w = 1 + \sum_{\mathcal{P}' \neq \mathcal{P}} \frac{2\mathrm{Re}(\mathcal{M}_{\mathcal{P}}\mathcal{M}^*_{\mathcal{P}'})}{|\mathcal{M}_{\mathcal{P}}|^2 + |\mathcal{M}_{\mathcal{P}'}|^2} \,. \tag{18}$$

The outer sum in Eq. (16) is as usual taken care of by generating many events.

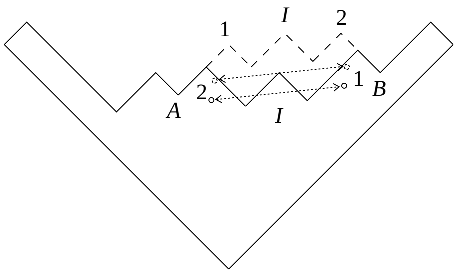

Fig. 3. The two possible ways, $(\ldots,1,I,2,\ldots)$ and $(\ldots,2,I,1,\ldots)$, drawn with solid and dashed lines respectively, to produce the entire state when two of the bosons are identical. The open circles show the two different production points for each identical boson and the arrows indicate the space-time difference, δx, between the two production points for the two production configurations. A and B denote the two vertices surrounding the identical bosons.

In order to see the main feature of symmetrising the hadron production amplitude in the Lund Model we consider Fig. 3, in which two of the produced hadrons, denoted $(1,2)$, are assumed to be identical bosons and the state in between them is denoted I. We note that there are two different ways to produce the entire state corresponding to the production configurations $(\ldots,1,I,2,\ldots)$ and $(\ldots,2,I,1,\ldots)$,*i.e.* to exchanging the two identical bosons. The two production configurations are shown in the figure and the main observation is that they in general correspond to different areas!

The area difference, ΔA, depends only on the energy momentum vectors p_1, p_2 and p_I, but can in a dimension-less and intuitively useful way be written

$$\frac{\Delta A}{2\kappa} = \delta p \delta x \,, \tag{19}$$

where $\delta p = p_2 - p_1$ and $\delta x = (\delta t; 0, 0, \delta z)$ is a reasonable estimate of the space-time difference, along the surface area, between the production points of the two identical bosons. We note that the space-time difference δx is always space-like. In Fig. 3 δx, for the two production configurations, is indicated by arrows, together with open circles showing the corresponding production points. The production points are in this way defined by the centres of the particles space-time rectangles.

We go on to consider the effects of transverse momentum generation in the $q\bar{q}$-vertices. First we note that the total transverse momenta of the sub-state $1, I, 2$ in Fig. 3 stem from the q and $\bar{q}$ generated at the two surrounding vertices, A and B. This is, owing to momentum conservation, fixed by the properties of the hadrons generated outside of the sub-state. Using this we find that there is a unique way to change the transverse momenta in the vertices surrounding the intermediate state I such that every hadron has the same transverse momenta in both production configurations.

Suppose as an example that we have generated $\pm\boldsymbol{k}_{\perp A}$ in the vertex A and $\pm\boldsymbol{k}_{\perp B}$ in the vertex B (*i.e.* so that $-\boldsymbol{k}_{\perp A}$ and $\boldsymbol{k}_{\perp B}$ defines the sub-state). Then to conserve the transverse momenta of the observed hadrons when changing production configuration from $(1, I, 2)$ to $(2, I, 1)$ it is necessary to change the generation of transverse momenta in the two vertices surrounding I as follows (in an easily understood notation):

$$\begin{aligned} \pm\boldsymbol{k}_{\perp I} &\to \pm(\boldsymbol{k}_{\perp A} + \boldsymbol{k}_{\perp B} - \boldsymbol{k}'_{\perp I})\,, \\ \pm\boldsymbol{k}'_{\perp I} &\to \pm(\boldsymbol{k}_{\perp A} + \boldsymbol{k}_{\perp B} - \boldsymbol{k}_{\perp I})\,. \end{aligned} \tag{20}$$

This means that exchanging two bosons with different transverse momenta will result in a change in the amplitude as given by Eq. (7) for some of the vertices.

From the amplitudes in Eq. (14) and Eq. (7) we get that the weight in the Lund Model can be written

$$w = 1 + \sum_{\mathcal{P}' \neq \mathcal{P}} \frac{\cos\dfrac{\Delta A}{2\kappa}}{\cosh\left(\dfrac{b\Delta A}{2} + \dfrac{\Delta(\sum p_{\perp q}^2)}{2\sigma_{p_\perp}^2}\right)}\,, \tag{21}$$

where Δ denotes the difference with respect to the configurations $\mathcal{P}$ and $\mathcal{P}'$ and the sum of $p_{\perp q}^2$ is over all vertices. We have introduced $\sigma_{p_\perp}$ as the width of the transverse momenta for the generated hadrons, (*i.e.* $\sigma_{p_\perp}^2 = 2\sigma^2$).

Using Eq. (19) for a single pair exchange one sees that the area difference is, for small δp, governed by the distance between the production points and that ΔA increases quickly with this distance. We also note that ΔA vanishes with the four-momentum difference and that the contribution to the weight from a given configuration, $\mathcal{P}'$, vanishes fast with increasing area difference ΔA.

From these considerations it is obvious that only exchanges of pairs with a small δp and a small δx will give a contribution to the weight. In this way it is possible to relate to the ordinary way to interpret the BEC effect, *cf.* Eq. (2).

It is straightforward to generalize Eq. (19) to higher order correlations. One notes in particular that the area difference does not vanish if more than two identical bosons are permuted and only two of the bosons have identical four-momenta.

Models for BEC have been suggested, *e.g.* [13], with similar weight functions, but it is important to note that the weight in this model has a scale both for the argument to the cos-function as well as for the function which works as a cut-off for large δp and δx (in our case a cosh-function). Further the two scales in the model are different and well-defined, at least phenomenologically.

5. Implementation and results

To calculate the weight for a general event, with multiplicity n, one has to go through $n_1!n_2!\dots n_N! - 1$ possible production configurations, where n_i is the number of particles of type i and there are N different kinds of bosons. For a general e^+e^--event at 90 GeV this is not possible from a computational point of view.

We know however that the vast majority of configurations will give large area differences and they will therefore not contribute to the weight. From basic group theory we know that every group can be partitioned into its classes and this also goes for the well-known permutation group. I will not go into the details but it is possible to define an "order" number for the classes. This can be defined so that the minimum length over which particles are moved by the permutation increases with the order and consequently the area differences also increase and the contributions quickly decrease. Nevertheless, there are plenty of configurations of low order which are also very small and this is not acceptable when taking computing time into account. We have therefore abandoned an expansion into the classes of the permutation group.

We have instead approximated the sum in Eq. (21) with a sum over configurations of all orders with significant contributions to the weight. This has been done by introducing *exchange-links* between particles. We have only taken into account interference with configurations where all particles are produced in positions from which there is a link to a particle's original production position. Defining a link matrix, $\mathcal{L}$, as follows

$$\mathcal{L}_{ij} = \begin{cases} 1 & \text{if there is a link between particles } i \text{ and } j, \\ 0 & \text{otherwise,} \end{cases}$$

one gets a simple representation of the configurations to be considered. The function of a link, $\mathcal{L}_{ij}$, is to enable moving particle i to particle j's position. It is important to note that a general link matrix enables higher order permutations even though the links are defined between pairs only. If all elements in $\mathcal{L}$ are 1, it corresponds to considering all $n!$ permutations, while only the original configuration is considered if $\mathcal{L}$ is the identity matrix.

We introduce the concept of link-size as the invariant four-momentum difference together with the invariant mass of the particles produced in between the pair (in rank). By only accepting links between particles if the size of the link between them is smaller than some cut-off link-size, δ_{c}, we get a prescription for the exchange matrix of an event.

In this way, by specifying the allowed two-particle exchanges, we get, to all orders, which configurations to take into account. We have found that for a given δ_{c} one includes all configurations that provide a contribution larger than some ϵ to the weight. Taken together this means that we get all the important contributions to the weight if we chose δ_{c} so large that the neglected terms smaller than ϵ give a negligible change for every weight.

We have used a cut-off link-size such that there is a link between identical bosons if one of the following conditions is fulfilled.

- $Q^2 = -(p_i - p_j)^2 < Q^2_{\mathrm{max}} \simeq 1\ \mathrm{GeV}^2$.
- the invariant mass of the particles produced in between (along the string) the pair is less than $m^2_{\mathrm{max}} \simeq (20\ \mathrm{GeV})^2$.

Including links larger than this give no contribution to the weight and no noticeable effect in any observable known to us (except the computing time in the simulation!).

In order to see the properties of the weight distribution I show in Fig. 4 that the majority of the weights are close to and centered around unity. There is also a tail of weights far away from unity in both directions. The tail of positive weights is shown as an insert and the distribution looks like a power. If we subdivide the events into sets with similar number of links and study the weight distributions for these sets separately, we find, however, that the weight distribution for each set is basically Gaussian. The width of these Gaussians increases with the number of links in the corresponding set, as shown in Fig. 5. The power like behaviour of the weight distribution is therefore merely a consequence of summing over events with different number of links. It should be emphasized that the negative weights only are a technical problem. Summing over many events results in positive probabilities for all physical observables, which is obvious from Eq. (16).

I have gone into some detail on the precise way of calculating in our model because I know that there is a large interest for similar calculations in the polish high-energy community. There is another problem related to

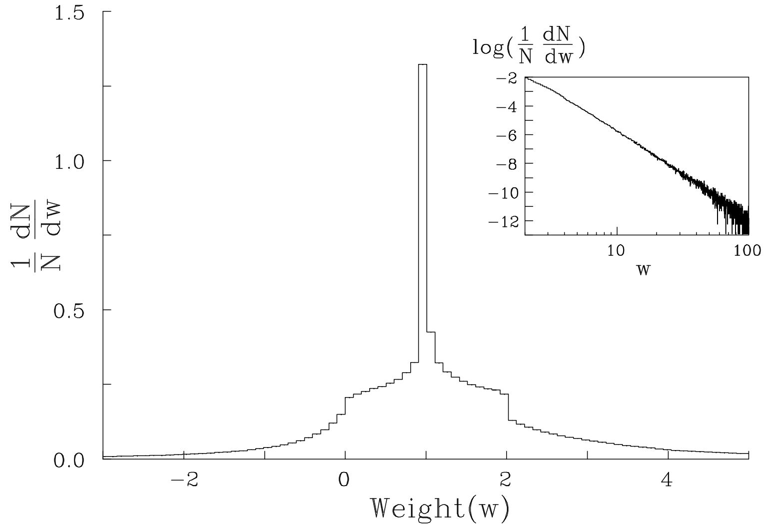

Fig. 4. The distribution of Bose–Einstein weights for two-jet states in JETSET. The tail of positive weights is shown in the insert.

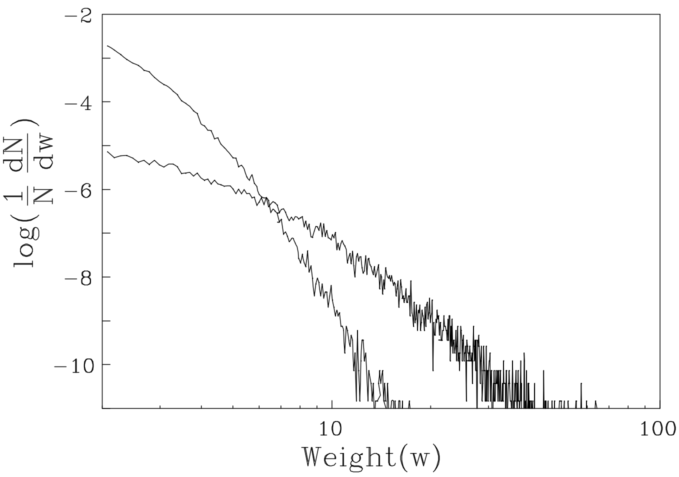

Fig. 5. The distribution of Bose–Einstein weights for two-jet events subdivided into sets with different number of links, n_l. Two samples for $3 \leq n_l \leq 5$ and $10 \leq n_l \leq 12$ are plotted.

the resonances and their decays. A large fraction of all final-state bosons stem from decays of short-lived resonances with lifetimes comparable to the time scale in string decay. Therefore they may contribute to the Bose–Einstein effect. To include their decay amplitudes and phase space factors and symmetrise the total amplitude is very difficult and it is furthermore not known how to do that in a model-consistent way. We have used a $\Gamma_{\rm min}$ so that particles with a width larger than $\Gamma_{\rm min}$ are assumed to decay before Bose–Einstein symmetrization sets in and the matrix elements are evaluated with their decay products regarded as being produced directly, ordered in rank.

Our results are fairly independent of $\Gamma_{\rm min}$ as long as it is small enough for the ρ's to decay before the symmetrization. It turns out, however, that the correlation function depends somewhat on the decay products of η'. The production rate of η' used in JETSET was questioned in [14], in connection with BE correlations. We have used reduced production rates for η and η' by setting the extra suppression factors in JETSET to 0.7 and 0.2 respectively, in accordance with the DELPHI tuning [18] and then our results are consistent with the ones presented at LEP.

From the basic ideas in the model and from Eqs (21) and (19) we may conclude that

- it is the transverse momentum fluctuations, which plays the role of "chaoticity" in this model
- the correlation length in Q depends inversely on the (space-like) distance between the production points of the identical bosons. Therefore the Bose–Einstein correlation length, that is dynamically implemented in this model, can be described as the flavour compensation length, *i.e.* the region over which a particular flavour is neutralized (along the color force field, *i.e.* the string).

It is then a natural prediction (which is also confirmed from our simulations) that there will be a different correlation length in "transverse" and "longitudinal" directions. These directions are then defined wrt. the thrust direction of the event and to be precise in the "longitudinal" cms frame, where the particles have opposite and equal longitudinal momentum components. Another obvious prediction, also noticeable in the model, is that neutral pions, that can be produced without any state I "in between" have a smaller longitudinal (coordinate space) correlation length than the charged pions where there must be a compensating charge state in between.

One could have hoped that kaon pairs should show a longer (coordinate space) correlation length but their very scarcity together with the well-known fact that they as decay products from resonances have larger transverse momentum than the corresponding pionic decay products means that there is no definite signal. Neither is it possible to use events with "many" kaons to obtain a longer pionic correlation length (the kaons are again too few to "crowd" the phase space).

Bose–Einstein correlations acting between identical bosons may have significant indirect effects on the phase space for pairs of non-identical bosons.

We have studied mass distributions of $\pi^+\pi^-$ systems to see how our model affects systems of unlike charged pions. Many analyses use $\pi^+\pi^-$ distributions to quantify the Bose–Einstein correlations, using the unlike-charged distributions as reference samples with which to compare the like-charged pion distributions. We have found that the assumption that the two-particle phase space densities for $\pi^+\pi^-$ systems are relatively unaffected by Bose–Einstein symmetrization is fairly good. Taking the ratio of the $\pi^+\pi^-$ mass distributions with and without Bose–Einstein symmetrization applied gives that the mass distribution is not altered much by the symmetrization, and that the effect is smaller than 5% in the entire mass range.

It has, however, been observed experimentally that the Breit–Wigner shape for oppositely charged pions in the decay of the ρ resonance [20–22] is distorted. We have therefore analysed $\pi^+\pi^-$ distributions when the pair comes from the decay of a ρ^0. We find that the weighting depletes the region around the ρ mass and shifts the masses towards lower values and there is also a slight increase in the width of the distribution in accordance with the experimental findings.

The existence of higher order dynamical correlations, which are not a consequence of two-particle correlations, is of importance for the understanding of BE correlations. There are very few experimental studies of genuine three-particle correlations, mainly because of the problem of subtracting the consequences of two-particle correlations and the need for high statistics of large multiplicity events. Genuine short-range three-particle correlations have been observed in e^+e^- annihilations by the DELPHI experiment. They conclude that they can be explained as a higher order Bose–Einstein effect [23].

A word of clarification is necessary here. In the BEC model of Sjöstrand, [5], there are also three-particle correlations due to the reshuffling to conserve the total energy-momentum. In our model three-particle correlations are inherent and actually, if the distributions again are divided into transverse and longitudinal ones serve to exhibit the string direction even further.

To reduce problems with pseudo-correlations due to the summation of events with different multiplicities we have used three-particle densities normalized to unity separately for every multiplicity in the following way

$$\tilde{\rho}_3^{(a,b,c)}(p_1,p_2,p_3) = \sum_{n\geq 8} P(n_a,n_b,n_c)\tilde{\rho}_3^{(n_a,n_b,n_c)}(p_1,p_2,p_3), \tag{22}$$

$$\tilde{\rho}_3^{(n_a,n_b,n_c)}(p_1,p_2,p_3) = \frac{1}{n_a(n_b-\delta_{ab})(n_c-\delta_{ac}-\delta_{bc})}\frac{1}{\sigma_{(n_a,n_b,n_c)}}\frac{d^3\sigma_{(n_a,n_b,n_c)}}{dp_1dp_2dp_3}, \tag{23}$$

where n is the charged multiplicity, σ_{n_a,n_b,n_c} is the semi-inclusive cross section for events with n_i particles of species i, and

$$P(n_a, n_b, n_c) = \frac{\sigma_{(n_a,n_b,n_c)}}{\sum_{n_a,n_b,n_c} \sigma_{(n_a,n_b,n_c)}} \,. \tag{24}$$

We have aimed to study the genuine normalized three particle correlation function, $\tilde{R}_3$, defined as

$$\begin{aligned} \tilde{R}_3 \;=\; & [\tilde{\rho}_3(p_1,p_2,p_3) - \tilde{\rho}_2(p_1,p_2)\tilde{\rho}_1(p_3) - \tilde{\rho}_2(p_1,p_3)\tilde{\rho}_1(p_2) - \tilde{\rho}_2(p_2,p_3)\tilde{\rho}_1(p_1) \\ & +2\tilde{\rho}_1(p_1)\tilde{\rho}_1(p_2)\tilde{\rho}_1(p_3)]/(\tilde{\rho}_1(p_1)\tilde{\rho}_1(p_2)\tilde{\rho}_1(p_3)) + 1 \,, \end{aligned} \tag{25}$$

where we have used an abbreviated notation for the $\tilde{\rho}_3$ from Eq. (22), and $\tilde{\rho}_1$ and $\tilde{\rho}_2$ are the corresponding one- and two-particle densities, normalized in accordance with Eq. (22) and Eq. (23). $\tilde{R}_3$ is equal to one if all three-particle correlations are consequences of two-particle correlations.

In order to calculate the $\tilde{\rho}_2\tilde{\rho}_1$ and $\tilde{\rho}_1\tilde{\rho}_1\tilde{\rho}_1$ terms in Eq. (25) the common experimental procedure is to mix tracks from different events. In order to minimize the computing time we have used combinations of charged pions in the following way to approximate Eq. (25)

$$\tilde{R}_3 \equiv \frac{\tilde{\rho}_{3w}^{(\pm,\pm,\pm)} - 3(\tilde{\rho}_{3w}^{(\pm,\pm,\mp)} - \tilde{\rho}_3^{(\pm,\pm,\mp)})}{\tilde{\rho}_3^{(\pm,\pm,\pm)}} \,, \tag{26}$$

where w, as previously, denotes weighted distributions. There are a couple of things to note in connection with Eq. (26). If there are genuine positive three-particle correlations for $(+\,+\,-)$ and $(-\,-\,+)$ combinations, as observed by the DELPHI collaboration [23] they will if they come from BE symmetrization contribute to the $\tilde{R}_3$ in Eq. (26), but they will reduce the signal. Secondly, we note that there is a possible bias from two-particle correlations from $(+-)$ combinations but that it is small as discussed previously. We also note that using the normalization in Eq. (23) reduces problems with contributions from like- and unlike-charge combinations having different multiplicity dependence. It should also be observed that the $\tilde{R}_3$ in Eq. (26) can be studied experimentally since getting the $\tilde{\rho}_{3w}$'s of course is achieved by analysing single events and the $\tilde{\rho}_3$ samples can be made by mixing events.

We have analysed the three-particle correlations as a function of the kinematical variable

$$Q = \sqrt{q_{12}^2 + q_{13}^2 + q_{23}^2} \quad \text{with} \quad q_{ij}^2 = -(p_i - p_j)^2 \tag{27}$$

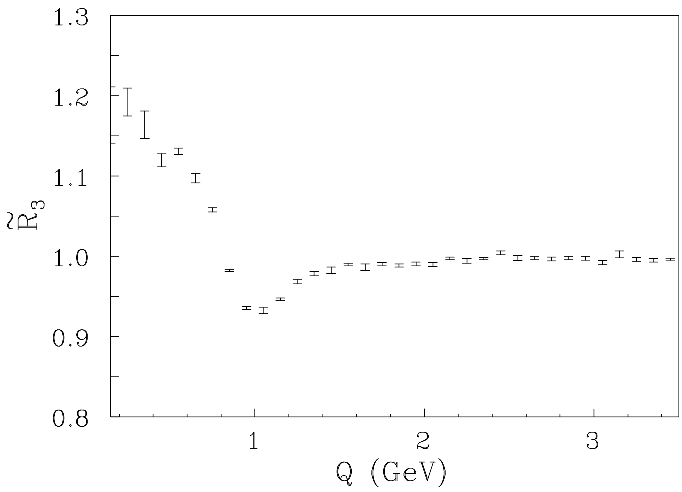

Fig. 6. The Q-dependence of the genuine three-particle correlation function $\tilde{R}_3$, defined in the text.

Fig. 6 shows $\tilde{R}_3$, the genuine three-particle correlation function for like-sign triplets, as approximated in Eq. (26). A strong correlation is observed for small Q-values. There is a dip in the curve for Q-values around 1 *GeV* which is compatible with the depletion of ρ^0's around its mass and gives an indication of the error from using unlike-charged pions in the approximation of $\tilde{R}_3$.

REFERENCES

[1] HERWIG 5.9; G. Marchesini, B.R. Webber, G. Abbiendi, I.G. Knowles, M.H. Seymour, L. Stanco, *Comput. Phys. Commun.* **67**, 465 (1992).

[2] T. Sjöstrand, *Comput. Phys. Commun.* **82**, 74 (1994).

[3] B. Andersson, G. Gustafson, G. Ingelman, T. Sjöstrand, *Phys. Rep.* **97**, 31 (1983).

[4] R. Hanbury-Brown, R.Q. Twiss, *Nature* **178**, 1046 (1956).

[5] L. Lönnblad, T. Sjöstrand, *Phys. Lett.* **B351**, 293 (1995).

[6] M.G. Bowler, *Z. Phys.* **C29**, 617 (1985).

[7] B. Andersson, W. Hofmann, *Phys. Lett.* **B169**, 364 (1986).

[8] B. Andersson, G. Gustafson, B. Söderberg, *Z. Phys.* **C20**, 317 (1983).

[9] N.K. Glendenning, T. Matsui, *Phys. Rev.* **D28**, 2890 (1983).

[10] J. Schwinger, *Phys. Rev.* **82**, 664 (1951).

[11] R. Kronig, *J. Amer. Optical Soc.* **12**, 547 (1926).; H.A. Kramers, *Atti del Congress Internationale de Fisici Como* (1927)

[12] B. Andersson, G. Gustafson, A. Nilsson, C. Sjögren, *Z. Phys.* **C49**, 79 (1991).

[13] S. Todorova, Private communications.

[14] M.G. Bowler, *Phys. Lett.* **B180**, 299 (1986).

[15] D. Decamp *et al.* (ALEPH Coll.), *Z. Phys.* **C54**, 75 (1992).

[16] P. Abreu *et al.* (DELPHI Coll.), *Z. Phys.* **C63**, 17 (1994).

[17] P.D. Acton *et al.* (OPAL Coll.), *Phys. Lett.* **B267**, 143 (1991).

[18] K. Hamacher, M. Weierstall, *DELPHI 95-80 PHYS 515* (1995)

[19] T. Alber *et al.*, (NA35 Coll.), *Z. Phys.* **C66**, 77 (1995).
H. Bøggild *et al.* (NA44 Coll.), *Phys. Rev. Lett.* **74**, 3340 (1995).

[20] P.D. Acton *et al.* (OPAL Coll.), *Z. Phys.* **C56**, 521 (1992).
P. Abreu *et al.* (DELPHI Coll.), *Z. Phys.* **C65**, 587 (1995).

[21] P. Abreu *et al.* (DELPHI Coll.), *Z. Phys.* **C63**, 17 (1994).

[22] G. Lafferty, *Z. Phys.* **C60**, 659 (1993).

[23] P. Abreu *et al.* (DELPHI Coll.), *Phys. Lett.* **B355**, 415 (1995).

[24] B. Lörstad, O.G. Smirnova, Proceedings of the 7th International Workshop on Multiparticle Production 'Correlations and Fluctuations', Nijmegen, The Netherlands 1996.